Volume 1 | Number 1 | Jan 2013 | Pages 1–100

Metallomics

Integrated biometal science
www.rsc.org/metallomics

ROYAL SOCIETY OF CHEMISTRY
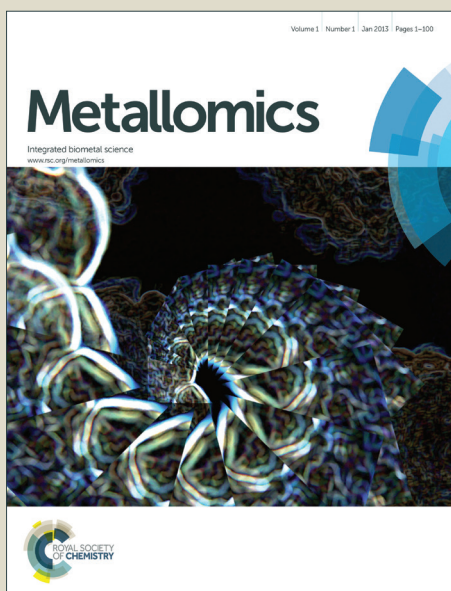
This is an *Accepted Manuscript*, which has been through the Royal Society of Chemistry peer review process and has been accepted for publication.

Accepted Manuscripts are published online shortly after acceptance, before technical editing, formatting and proof reading. Using this free service, authors can make their results available to the community, in citable form, before we publish the edited article. We will replace this *Accepted Manuscript* with the edited and formatted *Advance Article* as soon as it is available.

You can find more information about *Accepted Manuscripts* in the **Information for Authors**.

ROYAL SOCIETY OF CHEMISTRY

www.rsc.org/metallomics

Metallomics

PAPER

Inhibition of human amylin fibril formation by insulin-mimic vanadium complexes

Lei He, Xuesong Wang, Cong Zhao, Dengsen Zhu, Weihong Du*

Toxicity of amyloid-forming proteins can be linked to many degenerative and systemic diseases. Human islet amyloid polypeptide (hIAPP, amylin) has been associated with type II diabetes. Methods for efficient inhibition of amyloid fibril formation are highly clinically important. This study demonstrated significant inhibitory effects of six vanadium complexes on hIAPP aggregation. Vanadium complexes
10 have been used as insulin-mimic agents for diabetes treatment for many years, such as bis(maltolato)-oxovanadium (BMOV). Different biophysical methods were applied to investigate the interaction between V complexes and hIAPP. Results indicated that the selected compounds affected the peptide aggregation by different action modes and rescued the cytotoxicity induced by hIAPP. Both the high binding affinity and the ligand spatial effect on inhibiting hIAPP aggregation are significant. Although
15 some of these compounds undergo biotransformation under the conditions of the experiments, and the active species are not identified, it is understood that the effect results from a particular compound and its conversion products. Importantly, our work provided information on the effects of the selected V complexes on hIAPP and demonstrated multiple levels of effects of V complexes against amyloid-related disease.

Introduction

20 Abnormal protein aggregation and amyloid formation have critical functions in several intractable neurodegenerative and systemic diseases.[1-4] These diseases include Alzheimer's disease, Huntington's disease, Parkinson's disease, prion disorders, Lou
25 Gehrig's disease, and type II diabetes.[5-13] In the case of type II diabetes, amyloid deposits form in the pancreatic islets because of the misfolding of human islet amyloid polypeptide (hIAPP, amylin), a 37-residue peptide (KCNTATCATQRLANFLVH-SSNNFGAILSSTNVGSNTY). hIAPP is synthesized by the
30 pancreatic β-cells and co-secreted with insulin. It adopts a random coil structure in its soluble and native state.[14-16] The normal physiological functions of hIAPP as a hormone include regulation of gastric emptying, suppression of food intake, and control of glucose homeostasis.[17-18] However, its native structure
35 converts into a β-sheet conformation during the fibrillogenesis process. β-sheet formation drives amyloid assembly, and the aggregate form of hIAPP is postulated to have a crucial function in β-cell toxicity in the pathology of type II diabetes.[19] Studies have indicated the amyloid fibril formation of hIAPP using 2D
40 infrared spectroscopy, electroparamagnetic resonance, sum frequency generation spectroscopy, nuclear magnetic resonance, and other methods.[20-25] Therefore, inhibition of hIAPP aggregation is a theoretical approach to prevent β-cell toxicity and delay or prevent type II diabetes in predisposed subjects.
45 Developing inhibitors against amyloid formation has elicited significant attention because of mechanism studies in amyloid fibril formation and potential therapeutic use.[26-32] Two extremely

predominant classes of hIAPP inhibitors have been developed to restrain the aggregation and the cytotoxicity of the peptide. First,
50 the inhibitors consist of small peptide fragments derived from the target protein that contain hIAPP self-recognition domains, such as the hexapeptide SNNFGA (residues 20–25), the heptapeptide GAILSST (residues 24–30), and the modified peptide NF(N-Me)GA(N-Me)IL.[33-35] Second, the inhibitors consist of aromatic
55 organic compounds, such as Congo red, phenolsulfonphthalein and rifampicin, which bind to amyloid fibrils and suppress fibril formation.[36-38] In addition, several metal ions display effective inhibitory action on hIAPP fibril formation. Zinc ion shows a two-site mechanism for the inhibition of hIAPP amyloidogenesis,
60 whereas copper interacts with human amylin to form metallo-peptide complexes that prevent the amyloid from forming β-pleated sheets.[39-40] Studies have shown that metal complexes are used to inhibit fibril formation of amyloid peptides.[41-43] Aromatic ruthenium complexes display significant inhibitory effects against
65 hIAPP amyloidogenesis because of diplex contribution from both metal ion and ligand.[44] However, the metal inhibitors with better binding affinity, effective inhibition, and lower toxicity against hIAPP aggregation are still under study.

Vanadium(V) is considered in diabetes mellitus treatment
70 because it has been shown to lower glucose effects in diabetic humans since the 1890s.[45-47] The in vitro insulin-mimetic effect of V ions was confirmed later in 1979.[48-49] Given the better absorption, distribution, and excretion patterns, as well as low toxicity of V complexes compared with inorganic salts, they have
75 been widely investigated as chronic treatment alternatives for

diabetes.[50-54] Among these complexes, 3-hydroxy-2-methyl-4-pyrone (maltol) is suitable as a ligand for vanadyl ions and has passed phase I clinical trials.[55] V compounds mimic insulin action through alternative signaling pathways, which involve the inhibition of phosphorylation of insulin receptor substrate 1, protein kinase B, glycogen synthase kinase 3, and Forkhead box protein O1 (FOXO1), as well as the interaction between two non-insulin receptor tyrosine (Tyr) kinases.[56]

Considering that V can be used for diabetes treatment and potential inhibitory effects of metal complexes on amyloid peptides, this study used a series of V-based complexes to elucidate their interactions with hIAPP and inhibitive effects on hIAPP aggregation. Based on previous studies, the V complexes were selected with extensive π delocalization and steric effect against hIAPP fibril formation potentially.[44] Fig. 1 shows the molecular structures of six V complexes, which are insulin mimics.[57-61] Among them, complex **2** and its ethylmaltol analog have been used in clinical trials.[60] Complex **1** was selected because of its better absorption than **2**. The ligand of complex **3**, metformin, is oral hypoglycemic agents to treat type II diabetes mellitus.[59] The ligands of six complexes possess various steric effects, especially for complexes **4**, **5** and **6**. The present work studied the changes in the physicochemical properties of hIAPP induced by a particular compound and its conversion products. Moreover, the relationship between the ligand property and aggregation behavior of this active peptide was explored. The V complexes, which have been used as insulin mimic agents for many years, showed multiple levels of effects on hIAPP aggregation. This study will aid in discovering new therapy approaches using existing agents with more potential medicinal values.
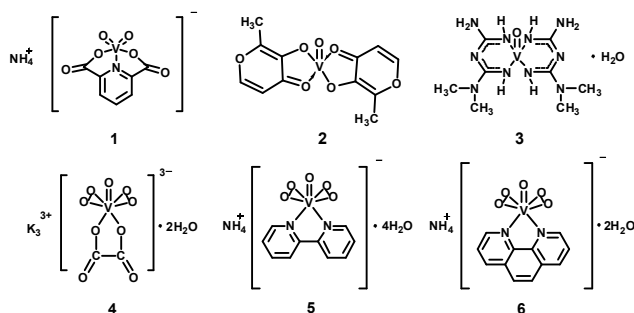

Fig. 1 Structures of Vanadium complexes: NH₄[V(O₂)(dipic)] **1**; BMOV **2**; VO(metf)₂·H₂O **3**; K₃[VO(O₂)₂(OX)]·2H₂O **4**; (NH₄)[VO(O₂)₂(bi-py)]·4H₂O **5**; (NH₄)[VO(O₂)₂(phen)]·2H₂O **6**.

Experimental section

Materials

hIAPP was chemically synthesized by GL Biochem Co., Ltd. (Shanghai, China) and further purified and identified by HPLC and MS. The sample purity was more than 95%. The metal complexes were prepared as described previously. All other reagents were of analytical grade. Lyophilized hIAPP was dissolved in hexafluoroisopropanol for 1 h to obtain a 4 mg/mL stock solution. Aliquots of the peptide stock solution were lyophilized before use.

Thioflavin T (ThT) assay

Fluorescence was monitored using an F-4500 fluorescence spectrometer (Hitachi, Japan) with a programmable temperature controller (PolyScience, USA). Metal compounds (50 μM) were added to 5 μM hIAPP in a 10 mM phosphate buffer at pH 7.5. The samples were incubated with 10 μM ThT, and the ThT signal was quantified by averaging the fluorescence emission at 484 nm over 10 s when the sample was excited at 432 nm. The final spectrum was obtained from the mean of the three repeated spectra. For the IC50 determination, the concentrations of V complexes were selected at 0, 1, 2, 3, 5, 10, 20, 30, and 50 μM, respectively. For the study of aggregation kinetics, the lyophilized peptide was dissolved in a 10 mM sodium phosphate buffer at pH 7.5 to a final concentration of 15 μM, and 150 μM of V compound was added to this solution. The emission intensity at 484 nm was measured from 0 h to 12 h.

Atomic force microscopy (AFM) images

Samples were prepared by adding the metal complexes to hIAPP solutions and incubated at 37 °C for 4 days. The final peptide concentration of all samples was 5 μM. Images were obtained in the tapping mode with a silicon tip under ambient conditions, a scanning rate of 1 Hz, and a scanning line of 512 using a Veeco D3100 instrument (Veeco Instruments 151 Inc., USA).

Circular dichroism (CD) analysis

The CD spectra were obtained on a Jasco J-810 spectropolari-meter (Japan Spectroscopy, Japan). The samples were prepared in 5 mM phosphate buffer at pH 7.5. The final concentration of peptide was 50 μM and 0.5 mM for V complexes. A 1 mm quartz cell was used for all CD spectra. The spectra were recorded between 190 and 250 nm with 0.5 nm spectral step and 2 nm bandwidth. A scan rate of 100 nm min⁻¹ with 1 s response time was used. The relevant baseline was subtracted by running phosphate buffer alone or buffer containing the corresponding V complex as blank. The ellipticity of the CD spectra was expressed in millidegrees (mdeg). Each spectrum represents an average of three accumulated scans.

Spectrofluorometric measurements

To determine the binding affinities between V complexes and hIAPP, a published fluorescence-based approach was adopted to determine the dissociation constant (K_d).[62] The excitation wavelength of 275 was selected based on the earlier report, and K_d was determined from the plot of fluorescence intensity versus the V complex concentration using the following equation:

$$\Delta F = F_0 - F_L = \frac{F_0 - F_\alpha}{2P_0}\left\{K_d + P_0 + M - \left[\left(K_d + P_0 + M\right)^2 - 4P_0 M\right]^{\frac{1}{2}}\right\} \quad (1)$$

where F_0 and F_L are the measured fluorescence intensities of the peptide at 303 nm in the absence and presence of V complex, respectively. F_α is the maximum fluorescence quenching of the peptide, P_0 is for the initial concentration of the peptide, and M is the concentration of added V complex, which was varied in the range of 0 μM to 300 μM. The results were obtained from the mean of three repeated experiments.

Electrochemical measurements

Electrochemical measurements were conducted on Epsilon

Electrochemical Workstation (USA). A glassy carbon electrode and a platinum wire were used as the working and counter electrodes, respectively. All the potential values were reported with regard to the Ag/AgCl reference electrode. Before each experiment, the working electrode was polished with 0.3 μm alumina slurry and ultrasonic bath in ultrapure water. A 5 mM phosphate buffer at pH 7.5 was used as the supporting electrolyte. The final concentration of V complex was 0.5 mM, with the absence and presence of 50 μM hIAPP. The scan rate was set at 100 mV/s. Each spectrum represents an average of three accumulated scans.

Cell culture and 3-(4,5)-dimethyl-thiazolyl-2,5-diphenyl-tetra-zolium bromide (MTT) assay

INS-1 rat insulinoma cell line was obtained from Bogoo Biotech Co., Ltd. (Shanghai, China). Cells were grown in monolayer cultures in RPMI-1640 medium supplemented with 10% FBS, 2 mM/L L-glutamine, 100 U/mL penicillin, and 100 U/mL streptomycin at 37 °C in a humidified (5% CO_2, 95% air) atmosphere. The cells seeded in 96-well microplate at a density of 1×10^4 cells per well were cultured at 37 °C in a humidified atmosphere for 24 h and exposed to different treatments. After a 48 h reaction, the cells were incubated with 10 μL of MTT at 37 °C. The final peptide concentration was 15 μM. The absorbance of the final solution was recorded in a UV spectrophotometer at 570 nm. Each experiment was carried out in quadruplicate. The data were calculated as percentage of untreated control value.

Results

Synthesis of V complexes

In this study, six V complexes, namely, ammonium (2,6-pyridne-dicaroxylic)dioxovanadate (NH$_4$[V(O$_2$)(dipic)]) **(1)**, bis(malto-lato)oxovanadium (BMOV) **(2)**, bis(*N′*,*N′*-dimethylbiguanidato)-oxovanadium (VO(metf)$_2$·H$_2$O) **(3)**, potassium oxalatooxo-diperoxovanadate (K$_3$[VO(O$_2$)$_2$(ox)]·2H$_2$O) **(4)**, ammonium (2,2′-bipyridine)oxodiperoxovanadate ((NH$_4$)[VO(O$_2$)$_2$(bipy)]·4H$_2$O) **(5)** and ammonium (1,10-phenanthroline)oxodiperoxovanadate ((NH$_4$)[VO(O$_2$)$_2$(phen)]·2H$_2$O) **(6)**, were synthesized and identified according to the reported methods.[59, 63-65] Details of the synthesis are presented in the Supporting Information. The products were in accordance with the literature and used for latter investigation. The ligands of them are pyridine-2,6-dicarboxylic acid for **1**, maltol for **2**, metformin for **3**, oxalic acid for **4**, 2,2'-bipyridine for **5** and 1,10-phenanthroline monohydrate for **6** respectively.

ThT analysis of hIAPP aggregation

hIAPP may self-aggregate and form amyloid deposit, which is correlated with type II diabetes. Amyloid fibrils can be monitored by the fluorescence dye ThT as a marker. Fig. 2A shows that the fluorescence spectrum produced a strong signal when ThT bound to hIAPP. However, ThT fluorescence intensity noticeably decreased after incubation of V complexes with hIAPP, suggesting that fibril formation of hIAPP was affected. Among the six V complexes, **2** and **6** exhibited stronger inhibitory effects on hIAPP aggregation, whereas other complexes performed generic fluorescence quenching to the peptide. This result

indicates that the change of fluorescence intensity was induced by V complex interaction because these V complexes had no Ultraviolet-visible (UV) absorption at 484 nm (data not shown). Moreover, the influence of V complex on hIAPP aggregation was concentration dependent (Fig. 2B). Table 1 shows the IC50 for different V complexes. The method of IC50 was employed according to earlier inhibitors investigation on Aβ protein,[66-67] and **2** displayed the most significant inhibition with its IC50 at 5 μM. By contrast, the inhibitions of independent ligands (pyridine-2,6-dicarboxylic acid; maltol; metformin; oxalic acid; 2,2'-bipyridine; and 1,10-phenanthroline monohydrate for corresponding V complexes) on hIAPP aggregation were not as prominent as their metal complexes (Fig. S1). This finding indicates that the formation of metal complex with a bigger steric effect may result in stronger inhibitory effect on amyloid formation.
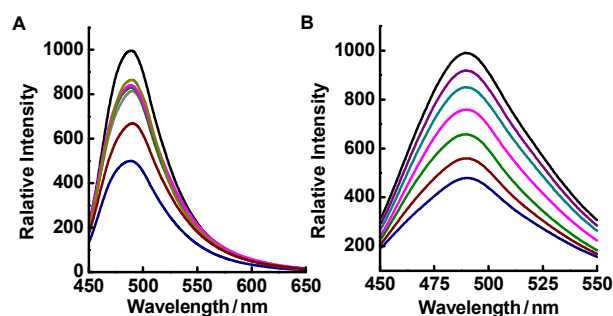

Fig. 2 Evaluation of the ability of V complexes to inhibit hIAPP aggregation as measured by ThT fluorescence (pH = 7.5). A) hIAPP was incubated with ThT in the absence (black) and presence of **1** (grey); **2** (blue); **3** (green); **4** (pink); **5** (yellow) and **6** (wine). B) The inhibitory effects of **2** on hIAPP (5 μM) aggregation. The concentrations of V complexes were 0, 1, 2, 3, 5, 10, 20, 30 and 50 μM respectively (from top to bottom).

Table 1 The IC50 value for the inhibition of vanadium complexes on hIAPP aggregation (pH = 7.5)

Vanadium complexes	Inhibition of fibril formation IC50 (μM) [a]
NH$_4$[V(O$_2$)(dipic)], **1**	8
BMOV, **2**	5
VO(metf)$_2$·H$_2$O, **3**	22
K$_3$[VO(O$_2$)$_2$(ox)]·2H$_2$O, **4**	15
(NH$_4$)[VO(O$_2$)$_2$(bipy)]·4H$_2$O, **5**	9
(NH$_4$)[VO(O$_2$)$_2$(phen)]·2H$_2$O, **6**	6

[a] Values were measured by the ThT fluorescence.

Amyloid formation rate decreased by V complexes

Amyloid fibrils are typically formed in a multistep process following a sigmoid growth model. This formation is highly dependent on the formation of energetically unfavorable nuclei. In the initial stage of aggregation prior to the formation of sufficient population of nuclei, amyloid formation proceeds very slowly, and only trace amounts of amyloid fibrils are formed. This process is known as the lag phase. The length of the lag phase indicates the relative stability of early intermediates in the aggregation process. The process aids in the assessment of

inhibitory effect of V complexes by monitoring the change in hIAPP aggregation kinetic profile. Fig. 3 shows a fibrillization process of hIAPP at 15 μM with a lag phase of approximately 2 h. This process was followed by a growth phase and a final plateau, in which fibrils were in equilibrium with soluble hIAPP. The system reached total equilibrium after 6 h. The plateau was delayed notably, and the observed signal intensity was lower than that of hIAPP alone in the presence of V complexes. The kinetic curves provided information on intense inhibitory effects of complexes **2** and **6** on hIAPP aggregation. It shows that hIAPP aggregation produced a lag phase of approximately 6 h in the presence of complex **6**, and the mixing system needed approximately 7.5 h to reach equilibrium. The plateau was approximately 50% lower than that of hIAPP alone. Incubation of **2** with hIAPP resulted in delayed lag phase (6.5 h), and the final plateau was delayed by approximately 8 h to reach equilibrium. The peak intensity was finally decreased by approximately 70%.
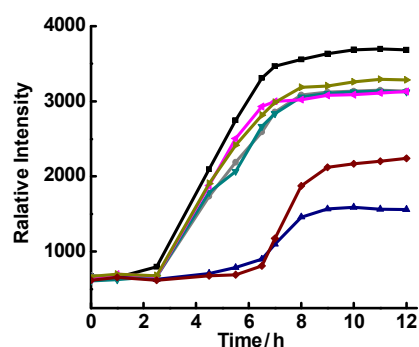

Fig. 3 ThT fluorescence monitored at 484 nm during hIAPP aggregation in the absence (black) and presence of **1** (grey); **2** (blue); **3** (green); **4** (pink); **5** (yellow) and **6** (wine) (pH = 7.5).

Morphology of amyloid deposition altered by V complexes

AFM was used to further confirm whether V complexes affected peptide aggregation and fibril formation. This technique has been used to determine different states of amyloidogenic peptides. Our previous study has verified that a fresh solution of hIAPP shows the absence of fibril formation.[44] However, after incubation, hIAPP (5 μM) displayed a remarkable fibril structure with a height of 60 nm to 80 nm (Fig. 4A). After incubation of V complexes (50 μM) with hIAPP, the mixing systems showed different patterns on the AFM images (Figs. 4B–4G). Compared with hIAPP, addition of **3** resulted in thin fibrils with a height of 40 nm to 50 nm. The presence of **5** influenced the aggregates of hIAPP more effectively than that of **3**, which resulted in the loose grid of non-rigid fibrils with a height of 30 nm to 40 nm. Furthermore, numerous flocculent deposits accompanied with a number of granular oligomers were detected in the presence of **4**. As shown in ThT fluorescence experiments, AFM images indicated the effect of complex **6** on hIAPP aggregation was stronger than that of other compounds. There had only several granular/spherical oligomers formed after hIAPP incubation. Moreover, minimal oligomers were observed in the case of **2**. As exhibited in the ThT assays, AFM images were also used to investigate the concentration-dependent characteristics of some complexes (Fig. S2). Similarly, the effects of the independent

ligands on hIAPP amyloid formation were not as noticeable as those in the corresponding V complexes (Fig. S3 and Figs. 4B–4G). This phenomenon indicates the better inhibitive effects of V complexes on peptide aggregation.
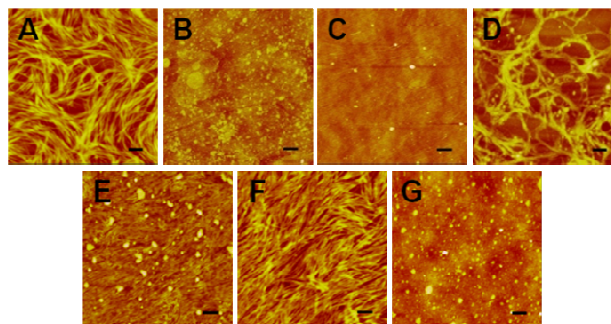

Fig. 4 AFM morphology of hIAPP fibrils in the absence (A) and presence of **1** (B); **2** (C); **3** (D); **4** (E); **5** (F) and **6** (G) (pH = 7.5).

hIAPP conformational transition changed by V complexes

hIAPP is a typical amyloid polypeptide, and the aberrant secondary structure β-sheet is responsible for fibril formation. CD spectroscopy was applied to investigate the effects of V complexes on the secondary structure transition of hIAPP. The negative CD signal at ~220 nm indicated that hIAPP could aggregate at a concentration of 50 μM after incubation at 37 °C for 96 h. This result implies that the β-sheet structure is the main component in the solution. After mixing V complexes with hIAPP and subtracting the absorption of corresponding V complex in phosphate buffer, the CD spectra of the system produced a negative signal at 198 nm, and the negative peak at 220 nm was weakened (Figs. 5 and S4). The influence of **4** on the CD spectra of hIAPP was noticeable at ~220 nm with an almost negligible signal at 198 nm. The mixing solution of **3** and hIAPP did not show a negative peak at 198 nm (Fig. S4). By contrast, the effect of **6** on the conformational transition of hIAPP was the most remarkable. Complex **2** and other V complexes also exhibited influences on the hIAPP solution conformation. The results illustrated that the β-sheet conformation of hIAPP is disrupted in the presence of V complexes.

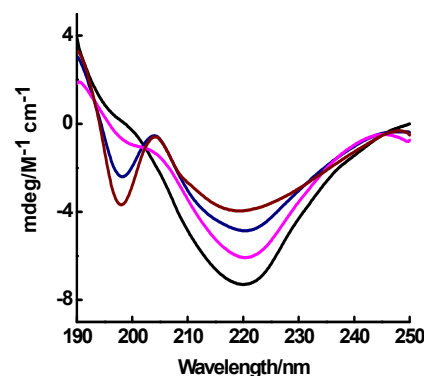

Fig. 5 CD spectra of hIAPP in the absence (black) and presence of **2** (blue), **4** (pink) and **6** (wine) (pH = 7.5). The spectra were smoothed by OriginPro software after subtracting the absorption of V complex.

Binding affinity between hIAPP and V complexes

To elucidate the interactions between hIAPP and V complexes, we used the method of intrinsic fluorescence quenching to calculate the dissociation constant K_d. The sensitive fluorescence 5 quenching of Tyr residue could represent structural changes caused by V complexes (Figs. S5 and 6). K_d was estimated by a nonlinear least-squares regression using Eq. 1 (see Experimental section). Table 2 shows the K_d value of different V complexes with hIAPP. Complex **6** showed the best binding affinity with the 10 K_d value of 6.0×10^{-6} M. The K_d values for **3** and **4** were 1.8×10^{-4} M and 1.4×10^{-4} M respectively, which were two order of magnitude larger than **6**. The K_d values for **2** and other V complexes binding to hIAPP were in the same order of magnitude of 10^{-5} M. These results were consistent with the CD experiments, 15 which suggest that V complexes showed different binding affinities to hIAPP.
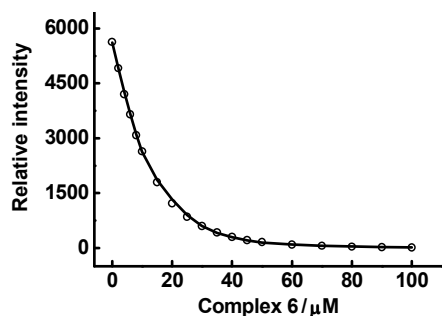

Fig. 6 Determination of K_d using the tyrosine fluorescence quenched by **6** (pH = 7.5). The circles are experimental data, and the curve is the fit 20 using eq1 with K_d of 6.0×10^{-6} M.

Table 2 K_d values for vanadium complexes with hIAPP (pH = 7.5)

Vanadium complexes	K_d ($\times 10^{-5}$ M) [a]
NH$_4$[V(O$_2$)(dipic)], **1**	3.3
BMOV, **2**	1.4
VO(metf)$_2$·H$_2$O, **3**	18.2
K$_3$[VO(O$_2$)$_2$(ox)]·2H$_2$O, **4**	13.9
(NH$_4$)[VO(O$_2$)$_2$(bipy)]·4H$_2$O, **5**	1.2
(NH$_4$)[VO(O$_2$)$_2$(phen)]·2H$_2$O, **6**	0.6

[a] Values were measured using the tyrosine fluorescence quenched by V complexes.

25

Cyclic voltammetric study of action modes of V complexes with hIAPP

The study of the interaction of macromolecule with small molecules is one of the applications of the electroanalytical 30 technique.[68-72] Thus, voltammetric method was used in the present study to determine the interaction modes between V complexes and hIAPP. Vanadium has different oxidation states, and the most commonly encountered in biological systems are V^{IV} and V^{V}. Both of them undergo very complex chemistry in 35 aqueous solution, forming a range of V species.[73] Besides, the solution redox chemistry of vanadium is complex and very sensitive to pH, metal concentration, and the presence of oxygen or other ligands.[51, 73-77]

    The cyclic voltammogram behavior of V complexes in the 40 absence and presence of hIAPP was recorded in Figs. 7 and S6 and listed in Table 3. Solution of complex **2** showed oxidative and reductive peak currents at approximately 0.47 V and 0.25 V, respectively. The addition of hIAPP resulted in significant decrease of both of these peaks, which suggests the formation of 45 a non-electroactive complex composed of hIAPP and V species that derived from complex **2**. Furthermore, the oxidative peak potential noticeably shifted from 0.47 V to 0.60 V, which was attributed to hydrophobic interaction between V species and hIAPP (Fig. 7A). Complex **6** showed a similar phenomenon as **2**. 50 For the solutions of **1** and **5**, the oxidative peak potential shifted a little toward higher potential without any changes in the current intensity after hIAPP addition. This finding indicates a weaker interaction between the hIAPP and V species which derived from **1** and **5**, respectively. However, the cyclic voltammogram of **4** 55 showed that the reductive peak shifted toward lower potential after hIAPP addition. This shift indicates the electrostatic interaction between hIAPP and the V species derived from **4** because of the more net charge that **4** possessed compared with other V complexes (Fig. 7B). Complex **3** showed that cyclic 60 voltammograms exhibited no change in both peak current intensity and peak potential. This finding implies the indistinctive interaction between hIAPP and V species of **3** (Fig. S6B) and it is in agreement with the observation detected by other methods. The electrochemistry results revealed that V species derived from 65 different V complexes could interact with hIAPP by different action modes.

Table 3 Cyclic voltammograms behaviour of V complexes (pH = 7.5) in the absence and presence of hIAPP obtained at glassy carbon electrode

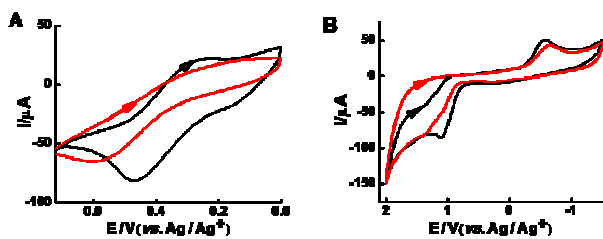| Solution of Vcomplexes	In the absence of hIAPP				In the presence of hIAPP			
	E_{pa}/V	E_{pc}/V	I_{pa}/μA	I_{pc}/μA	E_{pa}/V	E_{pc}/V	I_{pa}/μA	I_{pc}/μA
NH$_4$[V(O$_2$)(dipic)], **1**	0.67	-0.50	-39.80	19.40	0.85	-0.11	-48.55	13.75
BMOV, **2**	0.47	0.25	-82.04	21.54	0.60	-	-65.23	-
VO(metf)$_2$·H$_2$O, **3**	1.08	-	-68.75	-	1.07	-	-76.96	-
	-1.18	-	-19.71	-	-1.19	-	-18.99	-
K$_3$[VO(O$_2$)$_2$(ox)]·2H$_2$O, **4**	1.12	0.96	-86.36	-0.56	-	-	-	-
	-	-0.58	-	51.44	-	-0.65	-	42.8
(NH$_4$)[VO(O$_2$)$_2$(bipy)]·4H$_2$O, **5**	-0.99	-0.62	-28.41	24.33	-	-0.53	-	
	0.22		-12.54		0.39		-15.07	21.80
(NH$_4$)[VO(O$_2$)$_2$(phen)]·2H$_2$O, **6**	1.07	0.84	-36.95	0.40	-	-	-	-
	0.22	-0.02	-7.52	9.11	0.27	-	-5.61	-
	-0.25	-0.56	-2.89	31.74	-	-0.57	-	20.00

Fig. 7 Cyclic voltammograms of V complexes (pH = 7.5) in the absence (black line) and presence (red line) of hIAPP obtained at glassy carbon electrode for V complex **2** (A) and **4** (B), respectively.

Cytotoxicity of hIAPP regulated by V complexes

As previously described, V complexes interacted with hIAPP with better binding affinity, interfered with the peptide fibril formation, and resulted in the conformational transition of hIAPP. To determine their ability to inhibit the cytotoxicity induced by hIAPP, MTT reduction assay was performed using INS-1 insulinoma cells. Cell survival was evaluated after treating INS-1 cells with hIAPP alone or with the incubated peptide and V complex together. Compared with the control sample, hIAPP caused a significant reduction in cell viability to (46 ± 0.2) % (Fig. 8). V complexes showed lower cytotoxicity to INS-1 insulinoma cells themselves (Fig. S7). Moreover, the incubation of these complexes with hIAPP restored and upregulated cell viability (p <0.01) (Fig. 8). With the incubation of complexes **2** and **6**, it showed significantly decrease of cytotoxicity induced by the peptide, which results in the increase of cell viability to (87 ± 0.5) % and (81 ± 0.3) %, respectively. The other V complexes also decreased hIAPP cytotoxicity, with cell viability increasing to (72 ± 1.6) % for **4**, (70 ± 0.8) % for **1**, and (63 ± 0.5) % for **3**, despite being less active than **2**. However, **5** showed a little increase in the INS-1 insulinoma cell viability.
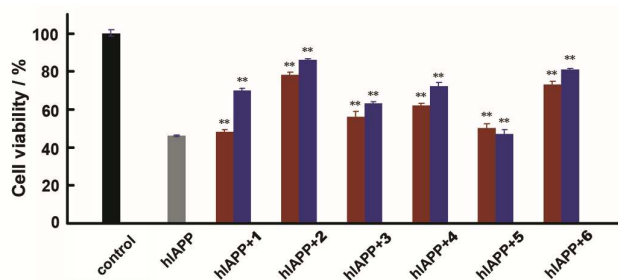

Fig. 8 Cell viability was monitored using the MTT assay. INS-1 cells were treated with (grey) or without hIAPP (15 μM, pH = 7.5) (black), or treated with hIAPP and different concentrations of V complexes, at 1.5 μM (red column) and 15 μM (blue column) respectively. The data are shown as means ± SD, n=3. **p $<$ 0.01 $vs.$ hIAPP (by Student's test)

Discussion

Significant efforts have been carried out to investigate the insulin-mimic properties of V complexes for type II diabetes treatment for many years, and **2** has entered into the clinical stage.[48-55, 57-61] However, the highly amyloidogenic protein hIAPP is also found in islet cells of patients with type II diabetes.

Several studies were conducted to investigate efficient drugs for the inhibition of hIAPP aggregation, but no study indicated an interaction between V compounds and hIAPP. The present work provides valuable informations about the inhibitory effects of V complexes on hIAPP, and demonstrates that the binding affinity and ligand spatial effect are important for the inhibition of hIAPP fibril formation.

Effective inhibition of V complexes on hIAPP aggregation

V complexes increase Tyr phosphorylation of the insulin receptor and other key insulin signaling proteins. They also increase membrane translocation of GLUT-4 glucose transporter in cultured cells for diabetes treatment.[78] This study used V complexes to target amyloid polypeptide hIAPP, which is associated with type II diabetes. As we know, some of these compounds undergo biotransformation under the conditions of the experiments, the application of vanadium-based drugs will generate multiple and variable active compounds resulting from hydrolysis and redox reaction.[73-74, 79] Although the active species are not identified in the present work, it is understood that these conversion products interacted and affected the aggregation properties of the peptide.

ThT assay and kinetic profile showed that all the active V complexes reversed the fibril formation. Moreover, the large ligand-containing complexes, such as **2** and **6**, exerted a stronger inhibitive effect on hIAPP aggregation by increasing the length of the lag phase and diminishing the aggregation degree of the peptide. The presented inhibitive effects are in the order of **2** $>$ **6** $>$ **1** $\approx$ **4** $\approx$ **5** $\approx$ **3**. IC50 values were also determined to further elucidate the inhibition efficiency of different V complexes and their derived active species on hIAPP aggregation. Compared with metal inhibitors of Aβ protein,[62] four of the V complexes had lower IC50 values under 10 μM. Notably, the IC50 values to the two strongest inhibitors **2** and **6** were 5 and 6 μM, respectively, which indicate a high-efficiency inhibition of the two compounds. An exception is complex **5.** It showed higher binding affinity and notable IC50 to hIAPP, but unsatisfactory image and cytotoxicity, which will be discussed later.

AFM images also illustrated that hIAPP fibrils with thick shape in the absence of V complexes could be scattered to filamentous aggregates and bits of oligomers when incubated with V complexes. Complex **2** showed the best inhibition with scarce granular oligomers, which was consistent with the ThT result. However the four compounds, **1**, **3**, **4**, and **5**, which had a relatively similar inhibitory effect in ThT assay showed different morphologies when detected by AFM.

To clarify, analyzing different properties of these compounds in solution is necessary. Among the six V complexes, two are traditional coordination complexes that may undergo hydrolysis and/or redox chemistry in a biological environment. Three peroxocomplexes will also undergo hydrolysis and redox chemistry.[73-74, 80] Complex **1** may form vanadate oligomers at pH 6.5 and above,[77] and the hydrolysis of complex **3** is facile and a brown solution (of vanadyl hydroxide) results.[59] As for complex **2**, the stability of its hydrolysis was deduced from UV/vis spectra. In the region $3 < \mathrm{pH} < 8$, the spectra (and therefore the ligand environment around the VO^{2+} center) remained relatively constant, but it was slowly oxidized in aerobic water to $[VO_2(ma)_2]^-$.[64] In addition, three peroxocomplexes exhibit

different stability in solution. The 2,2'-bipyridine ligand of complex **5** dissociates after six hours, producing the bisperoxo-aqua species$[V(O)(O_2)_2(H_2O)_2]^-$, while complex **6** is relatively stable for more than two days in solution.[80] The complex chemistry of V complexes will lead to different active species and distinct binding modes to hIAPP.

Therefore, we may conclude that the different AFM results may be induced by different binding modes between hIAPP and active V species, which further influence hIAPP self-aggregation. The results revealed that the different physiochemical properties of hIAPP might be attributed to different hydrolysis and redox products of V complexes. **2** was the most effective inhibitor against hIAPP aggregation.

Function of coordinated ligands in affecting hIAPP aggregation

Fluorescence quenching study showed that not only **6** and **2**, but also **5** showed a high binding affinity to hIAPP. However, the inhibition of **5** on hIAPP fibril formation was not satisfactory by AFM detection. Previous studies have indicated that active V species can be formed from hydrolysis, redox reactions, as well as geometric isomerization reactions. The complex stability is linked with many factors, such as ionic strength, pH value and other properties of the environment. For example, complex **5** and **6** exhibit different stabilities in solution.[80] When dissolved in pH 6.8 phosphate buffer, **5** produces the bisperoxo-aqua species after 6 h, while **6** is stable for more than 2 days in solution. As a result, **5** is prone to ligand dissociation and subsequent conversion to monoperoxo species. Different species may result in different binding mode and further influence its capacity to inhibit the fibril formation of hIAPP.

On the other hand, the aggregation of hIAPP depends on its sequential specificity, and the hydrophobic C-terminal fragments from residues 20 to 29 are critical in β-sheet structure and fibril formation.[81-84] However, the fluorescence quenching assay is based on the emission peak intensity of Tyr37, which is at the C-terminal of hIAPP. The active species of **5** may bind near the terminal residue Tyr37 with high binding affinity and it doesn't work on the core fragment that is in charge of hIAPP aggregation. Thus, the inhibitive effect of **5** appeared unremarkable. This phenomenon is similar to the interaction between palladium complex Pd(en)Cl$_2$ and prion neuropeptide PrP106-126,[85] which indicates that ligand spatial effect rather the high binding affinity contributes to better inhibition on amyloid peptide aggregation. Unlike complex **5**, complex **6** exhibited both high binding affinity and efficient inhibition effect. As described above, complex **6** is quite stable when compared to **5**. It showed better inhibitory effect on the peptide aggregation with distinct ligand spatial effect. This result suggests that not only the property of coordinated ligands but also their stability may influence the interaction system.

Moreover, we studied the inhibitive effects of the individual ligand on hIAPP aggregation. Among the six ligands, 1,10-Phenanthroline (phen) exhibited the best inhibition on hIAPP by AFM detection, and the ligand maltol of **2** showed weaker effect with several fibrils (Fig. S3B). This result may be attributed to the steric effect of the phen ligand by occupying a larger space and inhibiting the interface stack of hydrophobic region from residues 22 to 29 of hIAPP. Compared with the individual ligand, the active species derived from metal complex **2**, which was composed of two maltol ligands, showed stronger steric effect on inhibiting hIAPP fibril formation. Although the active species of V complexes were not identified in the present work, based on the chemical properties of the complexes and different biological activities exerted by the complexes, we propose that the coordinated ligands had an important inhibitory function in the process of protein aggregation. In fact, it may be not only the high binding affinity but also the scale of ligand and their stability assisting V complexes in affecting the peptide aggregation.

Analysis of V complexes interacting with hIAPP

ThT assay and AFM images indicated inhibitive effects of V complexes on hIAPP fibril formation. Determination of Tyr fluorescence quenching indicated that **2** and **6** had better binding affinity to hIAPP. However, the interactions between hIAPP and V complexes need to be verified further. CD spectra showed that the secondary structure of the peptide was significantly changed after incubation with V complexes, with the typical β-sheet signal at 220 nm weakened and a negative absorption at 198 nm appeared in some compounds, such as **1**, **2**, **5**, and **6**. The changes in CD spectra illustrated a significant conformational transition of hIAPP and significant interactions between V complexes and the peptide.

The cyclic voltammograms of V complexes in the absence and presence of hIAPP exhibited different electrochemical trends, which may result from the different binding modes between V complexes and the peptide. The evident decrease at peak current of **2** and **6** after hIAPP addition indicated the formation of non-electroactive protein–metal complex.[68-69] The observed potential shift toward higher potential may be attributed to their hydrophobic interaction with hIAPP.[70] Complexes **1** and **5** exhibited a similar hydrophobic action mode but without any apparent changes in the current intensity. The aforementioned four compounds are composed of hydrophobic aromatic ligands; therefore, hydrophobic effects may have a predominating function when the active V species bind to hIAPP. Steric effect was again confirmed to affect hIAPP aggregation. By contrast, when **4** interacted with hIAPP, the system displayed a different electrochemical behavior with its potential shifted slightly lower. This finding might suggest that the active species of complex **4** bound to hIAPP mainly through electrostatic interaction.[71-72] Compared with the original V complexes $[VO(O_2)_2(phen)]^-$, $[VO(O_2)_2(bipy)]^-$, and other compounds used in this study, $[VO(O_2)_2(OX)]^{3-}$ possessed more net charge, which could well explain a disparate interaction mechanism. However, compound **3**, with a hydrophilic ligand and zero net charge, its conversion product displayed no change in cyclic voltammogram study. These results were consistent with ThT, AFM, and fluorescence quenching study, which indicated that both hydrophobic and electrostatic interactions affected hIAPP aggregation, and the large space obstacle of V complexes potentiated the inhibitory effect.

Several studies have indicated that when V complexes are dissolved in aqueous media to function, they may release V ions through ligand dissociation both *in vitro* and *in vivo*.[86-87] However, our MS results did not provide evidence for the direct coordination between the V ions and the peptide (data not shown).

The metal complexes displayed better inhibition on hIAPP aggregation than their corresponding independent ligand, especially for those complexes with large steric effect and better stability in solution. This result revealed that not only aromatic organic compounds act as hIAPP inhibitors, but also the insulin mimic agents, V-coordinated metal complexes, have remarkable effects on peptide aggregation and power the use of V compounds.

Conclusions

This study provides vital information on the inhibitory effects of selected V complexes on hIAPP fibril formation that is associated with type II diabetes. V complexes, accompanying with its derived active species, can interact with hIAPP through either hydrophobic or electrostatic interaction and inhibit peptide aggregation remarkably. Moreover, better binding affinity and larger ligand spatial effect are both crucial to inhibit hIAPP aggregation. Considering cytotoxicity, we investigated changes of cell viability to further confirm the effects of V complexes on hIAPP-induced cytotoxicity, which was correlated with type II diabetes. As expected, V complexes could well rescue the cytotoxicity in INS-1 insulinoma cells that induced by hIAPP. Particularly, the using of clinical drug BMOV had the best effect on reversing aggregation and reducing cytotoxicity. These results elucidated that the existing insulin-mimic agents may undergo another therapy route for type II diabetes treatment. Further studies are necessary to follow up this work onsimple vanadate salts and other free ligands for comparison, and elucidate potential roles of coordination chemistry in the effects of vanadium compounds against amyloid fibril formation. In addition, we will try to develop and design more V complexes based on their beneficial spatial conformation and low cytotoxicity. Overall, our results may be valuable in designing novel metallodrugs against amyloid-related diseases.

Acknowledgements

Notes and references

Department of Chemistry, Renmin University of China, Beijing, China.
*Tel : 8610-62512660, Email : whdu@chem.ruc.edu.cn*

† Electronic Supplementary Information (ESI) available: [Synthesis of vanadium complexes and Figs. S1-S7.]. See DOI: 10.1039/b000000x/

1. F. Chiti and C. M. Dobson, *Annu. Rev. Biochem.*, 2006, **75**, 333-366.
2. Y. Wang, J. Xu, L. Wang, B. Zhang and W. Du, *Chem. Eur. J.*, 2010, **16**, 13339-13342.
3. A. Aguzzi and T. O'Connor, *Nat. Rev. Drug. Discov.*, 2010, **9**, 237-248.
4. A. Laganowsky, C. Liu, M. R. Sawaya, J. P. Whitelegge, J. Park, M. Zhao, A. Pensalfini, A. B. Soriaga, M. Landau and P. K. Teng, *Science*, 2012, **335**, 1228-1231.
5. D. J. Selkoe, *Physiol. Rev.*, 2001, **81**, 741-766.
6. J. Hardy and D. J. Selkoe, *Science*, 2002, **297**, 353-356.
7. K. Conway, S. J. LEE, J. C. ROCHET, T. Ding, J. Harper, R. Williamson and P. Lansbury, *Ann. NY Acad. Sci.*, 2000, **920**, 42-45.
8. G. Forloni, N. Angeretti, R. Chiesa, E. Monzani, M. Salmona, O. Bugiani and F. Tagliavini, *Nature*, 1993, **362**, 543-546.
9. E. Scherzinger, A. Sittler, K. Schweiger, V. Heiser, R. Lurz, R. Hasenbank, G. P. Bates, H. Lehrach and E. E. Wanker, *Proc. Natl. Acad. Sci. USA*, 1999, **96**, 4604-4609.
10. S. S. Ray and P. T. Lansbury, *Proc. Natl. Acad. Sci. USA*, 2004, **101**, 5701-5702.
11. P. Westermark, C. Wernstedt, E. Wilander and K. Sletten, *Biochem. Biophys. Res. Commun.*, 1986, **140**, 827-831.
12. F. H. Epstein, J. W. Höppener, B. Ahrén and C. J. Lips, *New Engl. J. Med.*, 2000, **343**, 411-419.
13. G. Cooper, A. Willis, A. Clark, R. Turner, R. Sim and K. Reid, *Proc. Natl. Acad. Sci. USA*, 1987, **84**, 8628-8632.
14. I. Saraogi, J. A. Hebda, J. Becerril, L. A. Estroff, A. D. Miranker and A. D. Hamilton, *Angew. Chem.*, 2010, **122**, 748-751.
15. R. L. Hull, G. T. Westermark, P. Westermark and S. E. Kahn, *J. Clin. Endocrinol. Metab.*, 2004, **89**, 3629-3643.
16. J. J. Wiltzius, M. Landau, R. Nelson, M. R. Sawaya, M. I. Apostol, L. Goldschmidt, A. B. Soriaga, D. Cascio, K. Rajashankar and D. Eisenberg, *Nat. Struct. Mol. Biol.*, 2009, **16**, 973-978.
17. M. Anguiano, R. J. Nowak and P. T. Lansbury, *Biochemistry*, 2002, **41**, 11338-11343.
18. A. Mascioni, F. Porcelli, U. Ilangovan, A. Ramamoorthy and G. Veglia, *Biopolymers*, 2003, **69**, 29-41.
19. A. Lorenzo, B. Razzaboni, G. C. Weir and B. A. Yankner, *Nature*, 1994, **368**, 756-760.
20. F. Evers, C. Jeworrek, S. Tiemeyer, K. Weise, D. Sellin, M. Paulus, B. Struth, M. Tolan and R. Winter, *J. Am. Chem. Soc.*, 2009, **131**, 9516-9521.
21. L. Fu, G. Ma and E. C. Yan, *J. Am. Chem. Soc.*, 2010, **132**, 5405-5412.
22. R. Soong, J. R. Brender, P. M. Macdonald and A. Ramamoorthy, *J. Am. Chem. Soc.*, 2009, **131**, 7079-7085.
23. D. B. Strasfeld, Y. L. Ling, S.-H. Shim and M. T. Zanni, *J. Am. Chem. Soc.*, 2008, **130**, 6698-6699.
24. L. Wang, C. T. Middleton, S. Singh, A. S. Reddy, A. M. Woys, D. B. Strasfeld, P. Marek, D. P. Raleigh, J. J. de Pablo and M. T. Zanni, *J. Am. Chem. Soc.*, 2011, **133**, 16062-16071.
25. C. T. Middleton, P. Marek, P. Cao, C.-c. Chiu, S. Singh, A. M. Woys, J. J. de Pablo, D. P. Raleigh and M. T. Zanni, *Nat. Chem.*, 2012, **4**, 355-360.
26. J. J. Meier, R. Kayed, C.-Y. Lin, T. Gurlo, S. Jayasinghe, R. Langen, C. G. Glabe and P. C. Butler, *Am. J. Physiol. Endocrinol. Metab.*, 2006, **291**, E1317-E1324.
27. R. Mishra, D. Sellin, D. Radovan, A. Gohlke and R. Winter, *ChemBioChem*, 2009, **10**, 445-449.
28. L. Estrada and C. Soto, *Curr. Top. Med. Chem.*, 2007, **7**, 115-126.
29. K. L. Sciarretta, D. J. Gordon and S. C. Meredith, *Methods Enzymol.*, 2006, **413**, 273-312.
30. C. Soto, E. M. Sigurdsson, L. Morelli, R. A. Kumar, E. M. Castaño and B. Frangione, *Nat. Med.*, 1998, **4**, 822-826.
31. M. R. Nilsson, M. Driscoll and D. P. Raleigh, *Protein Sci.*, 2002, **11**, 342-349.
32. Y. Miura, K. Yasuda, K. Yamamoto, M. Koike, Y. Nishida and K. Kobayashi, *Biomacromolecules*, 2007, **8**, 2129-2134.
33. M. Tatarek-Nossol, L.-M. Yan, A. Schmauder, K. Tenidis, G. Westermark and A. Kapurniotu, *Chem. Biol.*, 2005, **12**, 797-809.
34. L. A. Scrocchi, Y. Chen, S. Waschuk, F. Wang, S. Cheung, A. A. Darabie, J. McLaurin and P. E. Fraser, *J. Mol. Biol.*, 2002, **318**, 697-706.
35. J. J. Wiltzius, S. A. Sievers, M. R. Sawaya, D. Cascio, D. Popov, C. Riekel and D. Eisenberg, *Protein Sci.*, 2008, **17**, 1467-1474.
36. Y. Porat, Y. Mazor, S. Efrat and E. Gazit, *Biochemistry*, 2004, **43**, 14454-14462.
37. S. Zraika, R. Hull, J. Udayasankar, K. Aston-Mourney, S. Subramanian, R. Kisilevsky, W. Szarek and S. Kahn, *Diabetologia*, 2009, **52**, 626-635.
38. J. A. Irwin, H. E. Wong and I. Kwon, *Biomacromolecules*, 2012, **14**, 264-274.
39. S. Salamekh, J. R. Brender, S.-J. Hyung, R. P. R. Nanga, S. Vivekanandan, B. T. Ruotolo and A. Ramamoorthy, *J. Mol. Biol.*, 2011, **410**, 294-306.

40. B. Ward, K. Walker and C. Exley, *J. Inorg. Biochem.*, 2008, **102**, 371-375.

41. G. Ma, F. Huang, X. Pu, L. Jia, T. Jiang, L. Li and Y. Liu, *Chem. Eur. J.*, 2011, **17**, 11657-11666.

42. K. J. Barnham, V. B. Kenche, G. D. Ciccotosto, D. P. Smith, D. J. Tew, X. Liu, K. Perez, G. A. Cranston, T. J. Johanssen and I. Volitakis, *Proc. Natl. Acad. Sci. USA*, 2008, **105**, 6813-6818.

43. X. Wang, L. He, C. Zhao, W. Du and J. Lin, *J. Biol. Inorg. Chem.*, 2013, **18**, 767-778.

44. L. He, X. Wang, C. Zhao, H. Wang and W. Du, *Metallomics*, 2013, **5**, 1599-1603.

45. A. Srivastava and M. Mehdi, *Diabet. Med.*, 2005, **22**, 2-13.

46. K. H. Thompson, J. Lichter, C. LeBel, M. C. Scaife, J. H. McNeill and C. Orvig, *J. Inorg. Biochem.*, 2009, **103**, 554-558.

47. K. H. Thompson and C. Orvig, *J. Inorg. Biochem.*, 2006, **100**, 1925-1935.

48. E. L. Tolman, E. Barris, M. Burns, A. Pansini and R. Partridge, *Life Sci.*, 1979, **25**, 1159-1164.

49. G. R. Willsky, K. Halvorsen, M. E. Godzala III, L.-H. Chi, M. J. Most, P. Kaszynski, D. C. Crans, A. B. Goldfine and P. J. Kostyniak, *Metallomics*, 2013, **5**, 1491-1502.

50. D. Rehder, *Future Med. Chem.*, 2012, **4**, 1823-1837.

51. D. Rehder, *Inorg. Chem. Commun.*, 2003, **6**, 604-617.

52. J. Gätjens, B. Meier, T. Kiss, E. M. Nagy, P. Buglyo, H. Sakurai, K. Kawabe and D. Rehder, Chem. Eur. J., 2003, 9, 4924-4935.

53. M. Li, W. Ding, J. J. Smee, B. Baruah, G. R. Willsky and D. C. Crans, *Biometals*, 2009, **22**, 895-905.

54. H. Sakurai, *Chem. Rec.*, 2002, **2**, 237-248.

55. T. Iglesias-González, C. Sánchez-González, M. Montes-Bayón, J. Llopis-González and A. Sanz-Medel, *Anal. Bioanal. Chem.*, 2012, **402**, 277-285.

56. G. Pandey, G. C. Jain and N. Mathur, *J. Mol. Pathophysiol.*, 2012, **1**, 63-76.

57. G. R. Willsky, L.-H. Chi, M. Godzala III, P. J. Kostyniak, J. J. Smee, A. M. Trujillo, J. A. Alfano, W. Ding, Z. Hu and D. C. Crans, *Coordin. Chem. Rev.*, 2011, **255**, 2258-2269.

58. B. I. Posner, R. Faure, J. W. Burgess, A. P. Bevan, D. Lachance, G. Zhang-Sun, I. G. Fantus, J. B. Ng, D. A. Hall and B. S. Lum, *J. Biol. Chem.*, 1994, **269**, 4596-4604.

59. L. C. Woo, V. G. Yuen, K. H. Thompson, J. H. McNeill and C. Orvig, *J. Inorg. Biochem.*, 1999, **76**, 251-257.

60. J. H. McNeill, V. Yuen, H. Hoveyda and C. Orvig, *J. Med. Chem.*, 1992, **35**, 1489-1491.

61. J. Yale, C. Vigeant, C. Nardolillo, Q. Chu, J.-Z. Yu, A. Shaver and B. Posner, in *Vanadium Compounds: Biochemical and Therapeutic Applications*, Springer, 1995, pp. 181-190.

62. D. Jiang, X. Li, R. Williams, S. Patel, L. Men, Y. Wang and F. Zhou, *Biochemistry*, 2009, **48**, 7939-7947.

63. K. Wieghardt, *Inorg. Chem.*, 1978, **17**, 57-64.

64. C. Orvig, P. Caravan, L. Gelmini, N. Glover, F. G. Herring, H. Li, J. H. McNeill, S. J. Rettig and I. A. Setyawati, *J. Am. Chem. Soc.*, 1995, **117**, 12759-12770.

65. N. Vuletić and C. Djordjević, *J. Chem. Soc., Dalton Trans.*, 1973, 1137-1141.

66. S. R. Byeon, J. H. Lee, J.-H. Sohn, D. C. Kim, K. J. Shin, K. H. Yoo, I. Mook-Jung, W. K. Lee and D. J. Kim, *Bioorg. Med. Chem. Lett.*, 2007, **17**, 1466-1470.

67. V. P. Chauhan, I. Ray, A. Chauhan, J. Wegiel and H. M. Wisniewski, *Neurochem. Res.*, 1997, **22**, 805-809.

68. N. Hui, X.-L. Niu, J.-Y. Han, W. Sun and K. Jiao, *Amino Acids*, 2010, **38**, 711-719.

69. M. F. Cerdá, L. Luzuriaga, M. Wörner and E. Méndez, *Int. J. Electrochem. Sci*, 2010, **5**, 1618-1633.

70. S. S. Kalanur, J. Seetharamappa and V. K. A. Kalalbandi, *J. Pharmaceut. Biomed. Anal.*, 2010, **53**, 660-666.

71. M. F. Cerdá, E. Méndez, G. Obal, C. Kremer, J. S. Gancheff and A. M. Castro Luna, *J. Inorg. Biochem.*, 2004, **98**, 238-244.

72. M. T. Carter, M. Rodriguez and A. J. Bard, *J. Am. Chem. Soc.*, 1989, **111**, 8901-8911.

73. D. C. Crans, K. A. Woll, K. Prusinskas, M. D. Johnson and E. Norkus, *Inorg. Chem.*, 2013, **52**, 12262-12275.

74. D. C. Crans, J. J. Smee, E. Gaidamauskas and L. Yang, *Chem. Rev.*, 2004, **104**, 849-902.

75. N. D. Chasteen, J. K. Grady and C. E. Holloway, *Inorg. Chem.*, 1986, **25**, 2754-2760.

76. D. C. Crans, B. Zhang, E. Gaidamauskas, A. D. Keramidas, G. R. Willsky and C. R. Roberts, *Inorg. Chem.*, 2010, **49**, 4245-4256.

77. D. C. Crans, L. Yang, T. Jakusch and T. Kiss, *Inorg. Chem.*, 2000, **39**, 4409-4416.

78. A. Levina and P. A. Lay, *Dalton Trans.*, 2011, **40**, 11675-11686.

79. D. C. Crans and T. J. Meade, *Inorg. Chem.*, 2013, **52**, 12181-12183.

80. J. H. Hwang, R. K. Larson and M. M. Abu-Omar, *Inorg. Chem.*, 2003, **42**, 7967-7977.

81. D. F. Moriarty and D. P. Raleigh, *Biochemistry*, 1999, **38**, 1811-1818.

82. K. Tenidis, M. Waldner, J. Bernhagen, W. Fischle, M. Bergmann, M. Weber, M.-L. Merkle, W. Voelter, H. Brunner and A. Kapurniotu, *J. Mol. Biol.*, 2000, **295**, 1055-1071.

83. J. Madine, E. Jack, P. G. Stockley, S. E. Radford, L. C. Serpell and D. A. Middleton, *J. Am. Chem. Soc.*, 2008, **130**, 14990-15001.

84. P. Westermark, U. Engström, K. H. Johnson, G. T. Westermark and C. Betsholtz, *Proc. Natl. Acad. Sci. USA*, 1990, **87**, 5036-5040.

85. Y. Wang, L. Feng, B. Zhang, X. Wang, C. Huang, Y. Li and W. Du, *Inorg. Chem.*, 2011, **50**, 4340-4348.

86. B. G. Lemons, D. T. Richens, A. Anderson, M. Sedgwick, D. C. Crans and M. D. Johnson, *New J. Chem.*, 2013, **37**, 75-81.

87. D. C. Crans, S. Schoeberl, E. Gaidamauskas, B. Baruah and D. A. Roess, *J. Biol. Inorg. Chem.*, 2011, **16**, 961-972.

Metallomics Accepted Manuscript
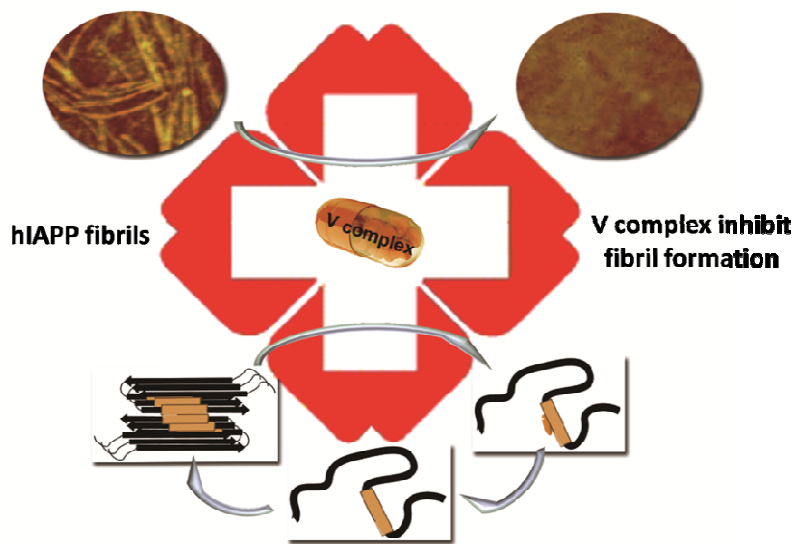
Graphic Abstract

Inhibition of human amylin fibril formation by insulin-mimic vanadium complexes

1
2
3
4
5
6
7
8
9
10
11
12
13
14
15
16
17
18
19
20
21
22
23
24
25
26
27
28
29
30
31
32
33
34
35
36
37
38
39
40
41
42
43
44
45
46
47
48
49
50
51
52
53
54
55
56
57
58
59
60

Graphic Abstract: Inhibition of human amylin fibril formation by insulin-mimic vanadium complexes
9x7mm (300 x 300 DPI)